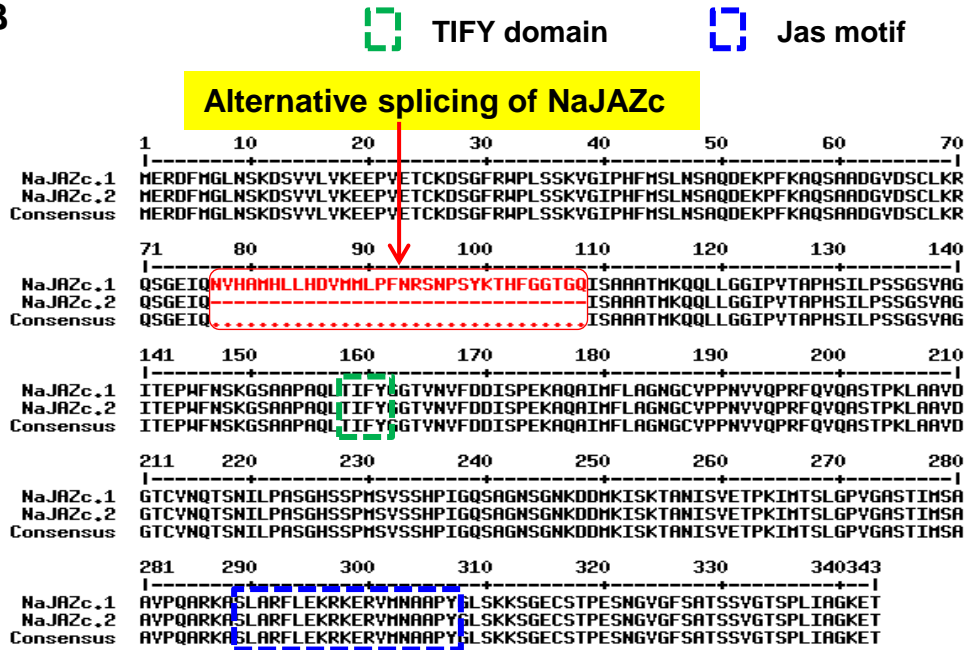
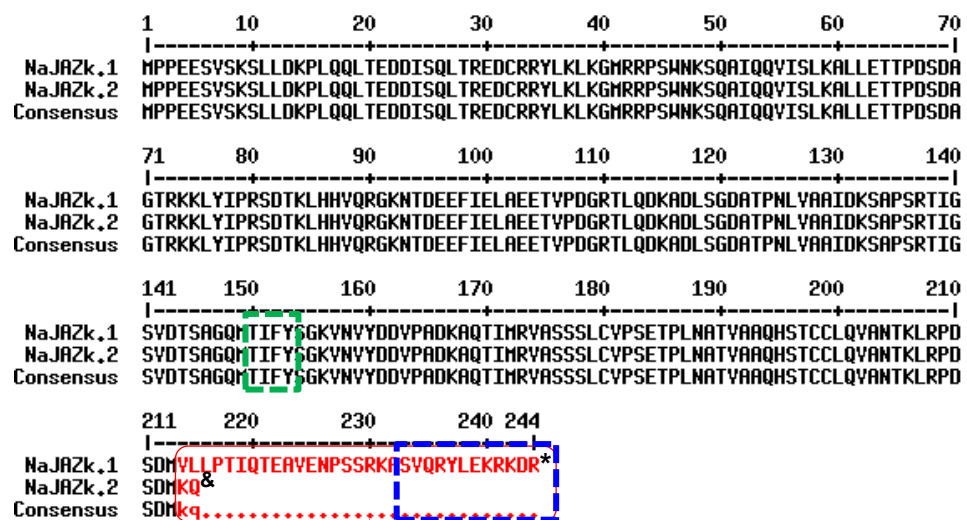


**A****B****C**

**Alternative splicing of NaJAZk and premature stop codon "\*"**

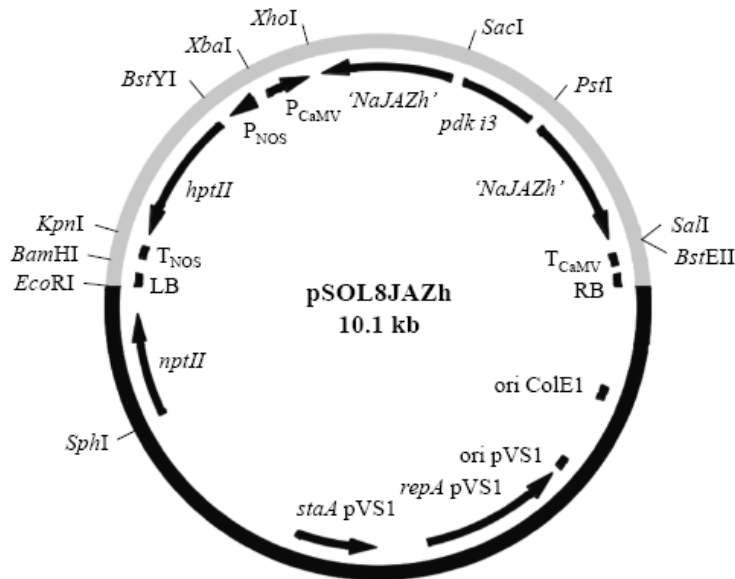
**Supplemental Figure S1.** Differential splicing of *NaJAZ* genes.

## Supplemental Figure S1 (continued)

(A) Primers outside differential sequences of NaJAZc and NaJAZk genes were designed to show the existence and relative ratios of alternatively spliced cDNA products. PCR products of differential length spanning the alternatively spliced regions of *NaJAZc* and *NaJAZk* genes were obtained in PCR reactions using cDNA templates of *N. attenuata* leaf samples. NaJAZc showed three bands of approximately the same intensity; NaJAZk produced two bands with a much stronger signal detected in a larger PCR product. (B) and (C) depict protein sequence alignments of the alternatively spliced forms of NaJAZc (NaJAZc.1, NaJAZc.2) and NaJAZk (NaJAZk.1 and NaJAZk.2) found during the cloning and sequencing of *N. attenuata* genes. NaJAZc.2 has 32 amino acid missing upstream of TIFY domain compared to NaJAZc.1 (B); NaJAZk.1 contains only a partial Jas motif (\*) while NaJAZk.2 lacks complete Jas domain (&).

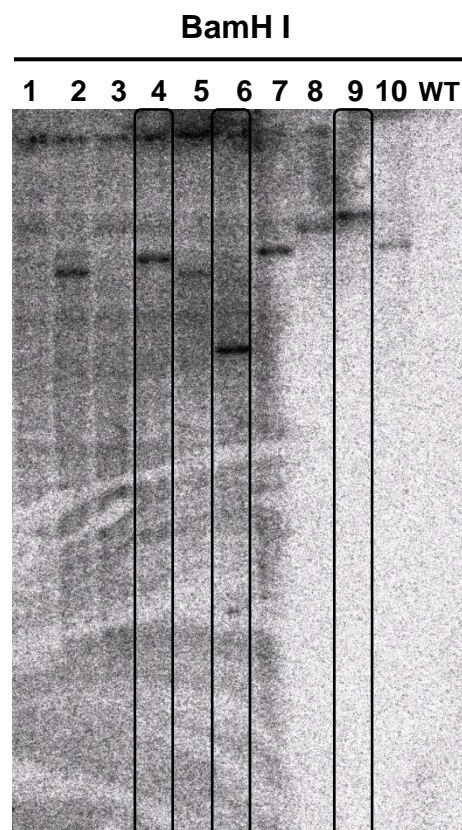
**A**

ATTTTCTTGTGATTTTTTAAAACATGTCAAATTCGCAAAATTCTTTTGACGGCGGCAGAAGGG  
 CCGGAAAAGCGCCGGAGAGATCGAATTTTCGTGCAGACTTGTAATTTATTGAGTCAGTTTATT  
 AAAGGAAAAGCTACTATTAGAGATCTGAATCTCGGAATTGCTGGAAAATCTGAAATCTCAGG  
 TAAAAGTGATGTTACAGAAGCTGCAACTATGGATTTATTGACAATTATGGAAAACCCCTCAA  
 TTGAAACTAAAGAACAAGAACAATAATCCATAGATCCCGTTTCGTGAGAGTGCTGTAACAGAA  
 TCTTCTAGAGATATGGAGGTGGCCGTAAATGAGCCCAGCACGAGCAAAGAGGCACCAAAAGA  
 GCCTAAGGCAGCACAAATTGACTATGTTCTATGATGGTAAAGTGATAGTATTTGATGATTTTC  
 CAGCTGACAAAGCTAGAGCAGTAATGTTATTGGCTAGTAAAGGATGCCCTCAGAGTTCATTT  
 GGCACTTTTTCATACTACAACCATCGACAAAATTAACACATCTGCTACTGCTGCTGCCACAGC  
 TTCTTTGACATGTAATAAACTAATCAGCTTAAACCAAGTACAGTTTCTATTGCACCACCAC  
 AACAAAAGCAGCAGCAAATTCATGTTTCTTATAGTAAAAGTGACCAACTCAAGCCAGGGTAT  
 AATTCTGCTACGCCGCAAGTACTGCAGCAGCAGCTAGTCCATGTTTCTAGTACTAGTAAAC  
 TGATCAGCTTAAGCCAGTATCAACTTCTTCTGCGTCGCAAAAACAGCAGGAGCAACATCAGC  
 AAACGCAGTCACAGACACCTGGAAGTAGCAGCTCTGAGCTACCTATTGCAAGAAGATCATCA  
 CTACATAGGTTTCTTGAGAAGAGGAAAGATAGGGCAACGGCTAGAGCGCCATACCAAGTTGT  
 ACATAATAATCCGTTACCATCATCTTCAAATAATAATGGGGAATCATCTTCCAAGGATTGCG  
 AAGATCAACTCGATCTCAATTTCAAGTTATAG

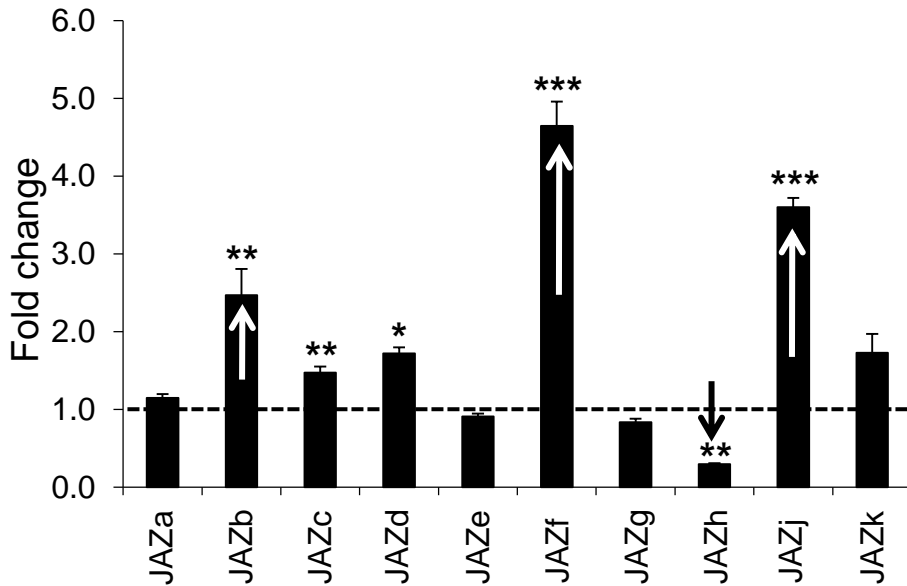
**B**

**Supplemental Figure S2.** NaJAZh sequence and vector used for plant transformation.

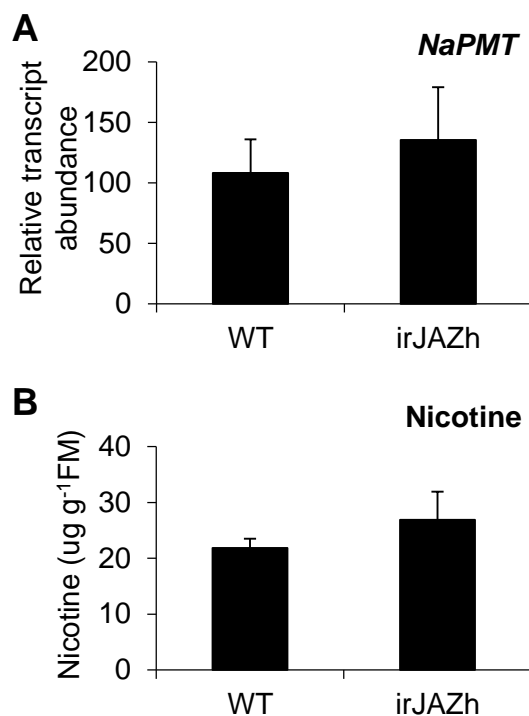
(A) Red letters show a 240bp region in the 3'UTR of *NaJAZh* that was used for gene silencing. (B) The pSOL8JAZH vector used for *Agrobacterium tumefaciens*-mediated transformation of *N. attenuata* plants.



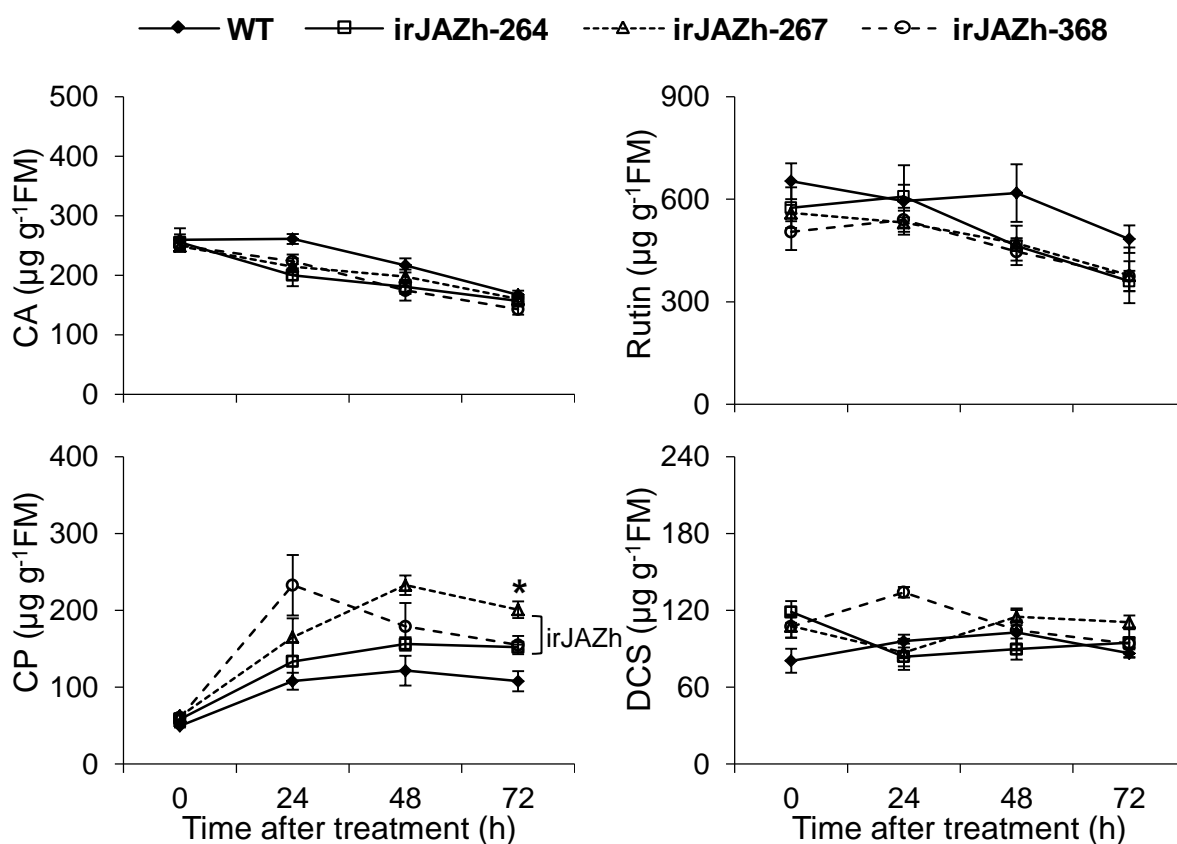
**Supplemental Figure S3.** Southern blot and number of T-DNA insertions in genomes of stable transgenic irJAZh lines. DNA gel blot of genomic DNA digested with BamHI enzyme from 10 independent irJAZh lines, hybridized with a probe coding for the hygromycin resistance gene located between right and left T-DNA borders of the transformation vector pSOL8JAZH. The black boxes indicate single insertion lines that were selected for further experiments: irJAZh-264 (loaded sample #4), -267 (sample #6) and -368 (sample #9).



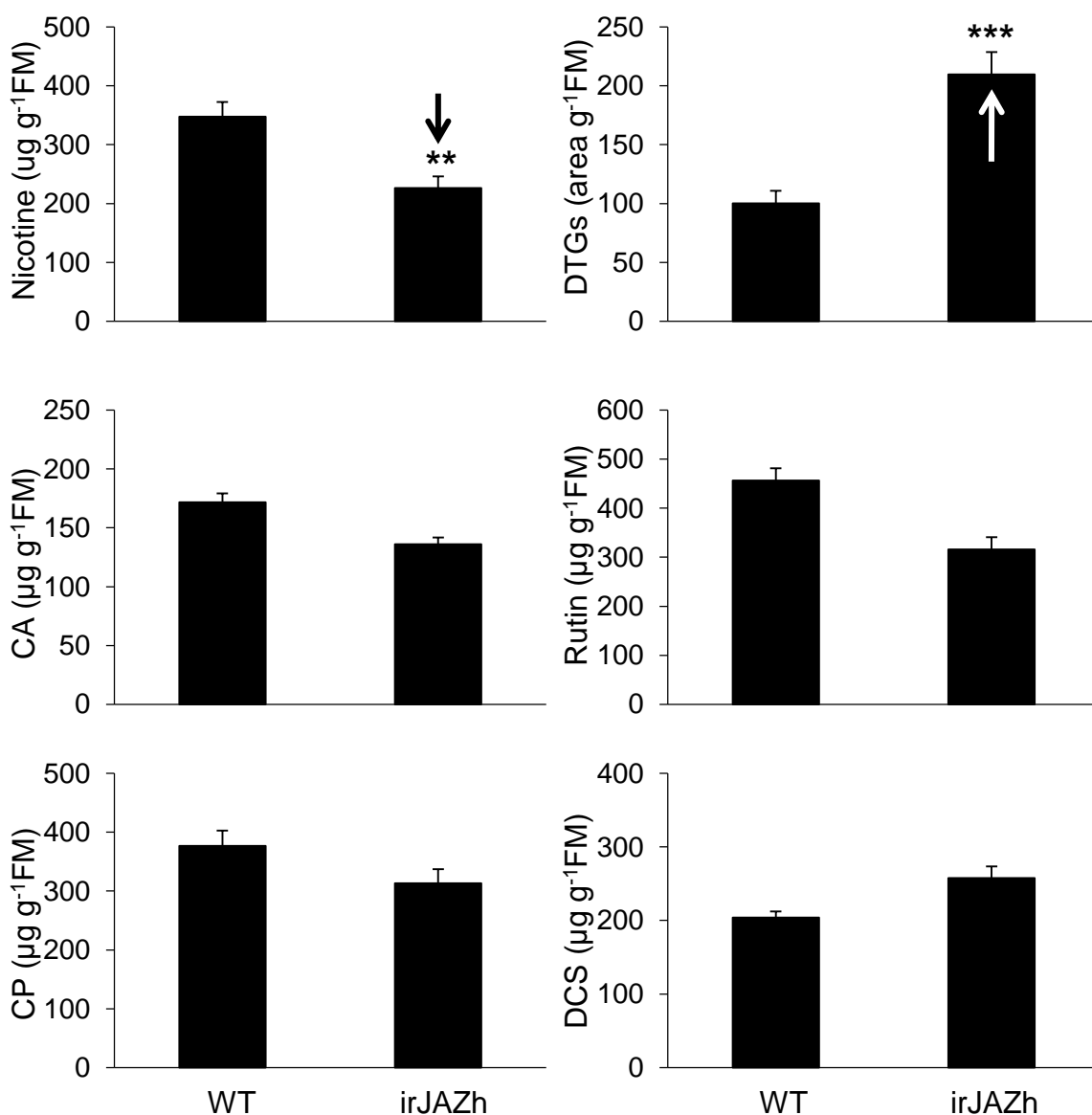
**Supplemental Figure S4.** Transcript levels of *NaJAZ* genes in irJAZh plants determined by microarrays. Fold changes (irJAZh-368/WT) of 10 *JAZ* genes in irJAZh leaves were determined by microarrays at 2 h after induction of the plants with simulated herbivory (W+OS); bars indicate fold changes  $\pm$  SE of 75 percentile-normalized microarrays signals ( $n=3$ ) in a single color (Cy-3) hybridization setup. Asterisks indicate significant differences between WT and irJAZh plants after W+OS treatment determined by Student's t-test (\* $P \leq 0.05$ , \*\* $P \leq 0.01$ , \*\*\* $P \leq 0.001$ ). *NaJAZl* and *NaJAZm* were not represented on the current version of the Agilent GPL13527 microarray platform and their expression is not shown.



**Supplemental Figure S5.** Nicotine levels and *NaPMT* gene expression in roots. (A) Expression levels of *N. attenuata* putrescine-N-methyltransferase (*NaPMT*) involved in nicotine biosynthesis and (B) nicotine content in roots of hydroponically-grown untreated irJAZh and WT plants ( $n=4$ ). Transcript abundances of *NaPMT* were determined by qPCR; nicotine content was determined by HPLC-PDA. No statistically significant differences were found between irJAZh and WT plants.

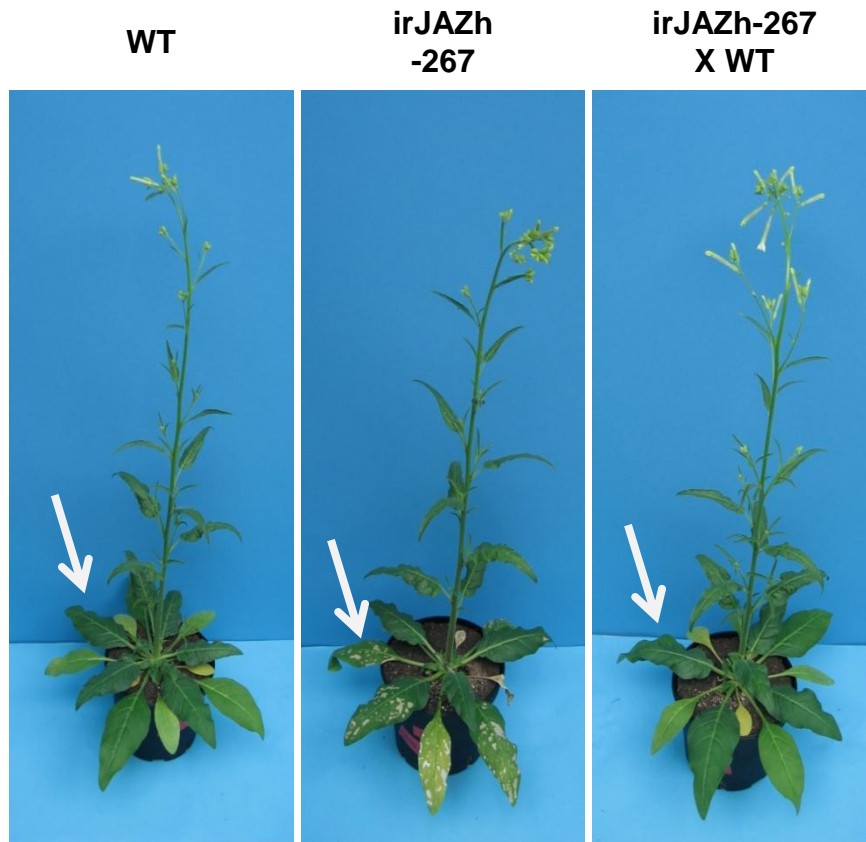


**Supplemental Figure S6.** Content of secondary metabolites in WT and irJAZh plants in the glasshouse. Rosette stage plants (WT; NaJAZh-silenced lines: irJAZh-264, -267 and -368) were treated with simulated herbivory (W+OS) and treated leaves were harvested before and 24, 48, and 72 h after elicitation. Mean  $\pm$  SE levels of chlorogenic acid (CA), rutin, caffeoylputrescine (CP) and dicaffeoylspermidine (DCS) were determined by HPLC coupled to PDA (Photo Diode Array) detector ( $n=3$ ). FM, fresh mass.

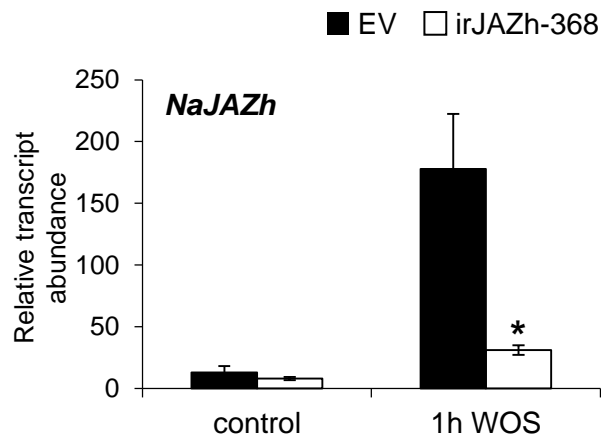


**Supplemental Figure S7.** Secondary metabolite levels in *M. sexta*-fed leaves from WT and irJAZh plants in the glasshouse. *M. sexta* neonates were placed on the leaf in the same position of each rosette plant. The leaves were then covered with transparent clip-cages to avoid caterpillar movement on the plant. After 5 days, *M. sexta* fed-leaves were harvested and analyzed for secondary metabolites by HPLC coupled to a combination of PDA/ELSD detectors; bars indicate level of secondary metabolites  $\pm$  SE ( $n=5$ ). Asterisks indicate statistically significant differences between WT and irJAZh plants after W+OS treatment determined by Student's t-test (\*\* $P \leq 0.01$ , \*\*\* $P \leq 0.001$ ). FM, fresh mass.

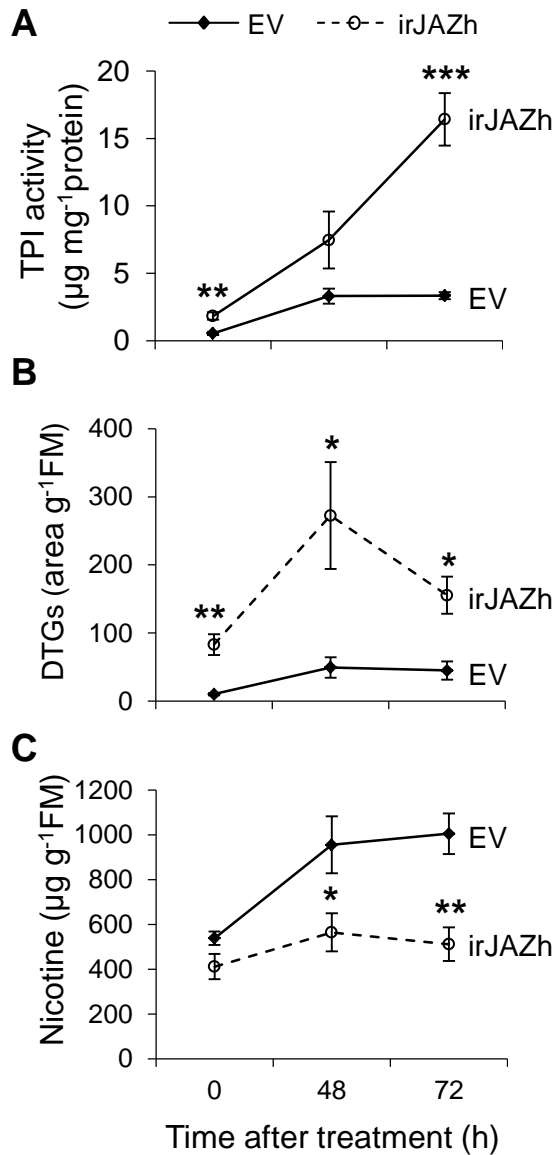




**Supplemental Figure S8.** Necrotic lesion symptoms of irJAZh plants were lost after crossing of homozygous irJAZh-267 with WT plants. The hemizygous irJAZh plants (right) do not show necrosis on their leaves compared to homozygous irJAZh-267 parents (middle) and resemble to WT plants (left); pictures of all plants were taken at 47 days after germination.

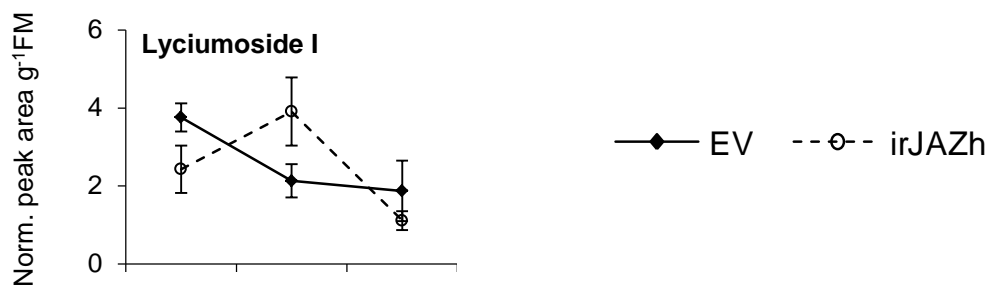


**Supplemental Figure S9.** Silencing efficiency of *NaJAZh* in field-grown EV and irJAZh plants. Transcript abundances of *NaJAZh* gene were determined by quantitative real time PCR (qPCR) in untreated (control) and 1 h W+OS-elicited (W+OS) leaves of EV and irJAZh plants ( $n=5$ ). Asterisks indicate significant differences between EV and irJAZh plants determined by Student's t-tests (\* $P\leq 0.05$ ).

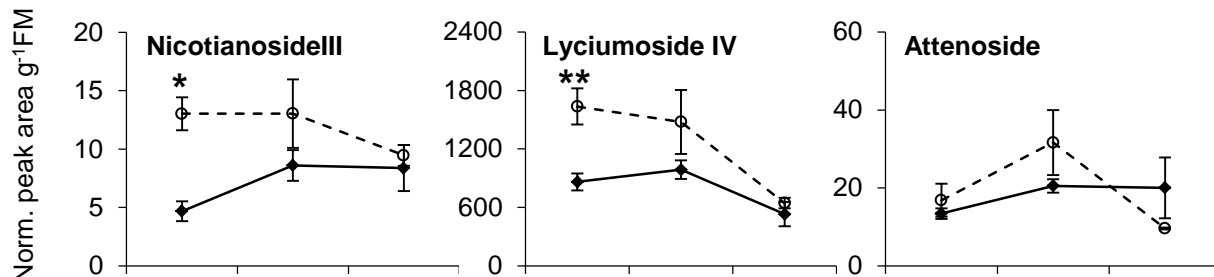


**Supplemental Figure S10.** Secondary metabolite levels determined in field-grown plants. (A) The activity of trypsin protease inhibitors (TPIs), content of (B) diterpene glycosides (DTGs) and (C) nicotine were determined in W+OS-elicited EV (empty vector) and NaJAZh-silenced plants in the native habitat in Great Basin Desert, Santa Clara, Utah, USA. Mean  $\pm$  SE levels of TPI activity and DTG accumulation in irJAZh plants ( $n=5$ ) were significantly higher compared to their levels in EV plants planted in a paired design in the same habitat. The levels of nicotine in irJAZh plants were significantly lower compared to EV plants ( $n=5$ ). Asterisks indicate significant differences between EV and irJAZh plants determined by Student's t-tests at each individual time point of measurement (\* $P \leq 0.05$ , \*\* $P \leq 0.01$ , \*\*\* $P \leq 0.001$ ). FM, fresh mass.

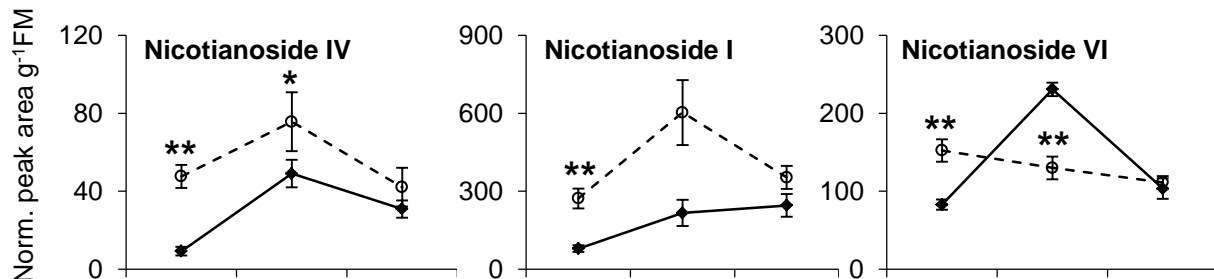
## 1. Precursor DTG



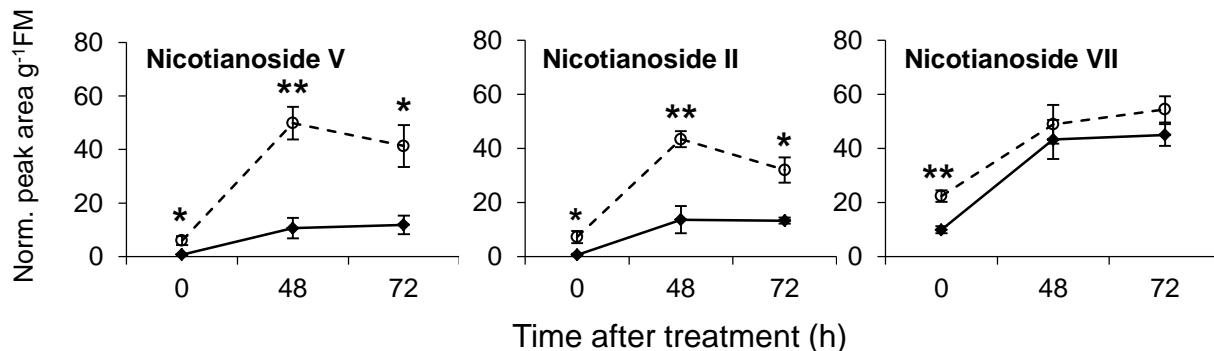
## 2. Core DTGs



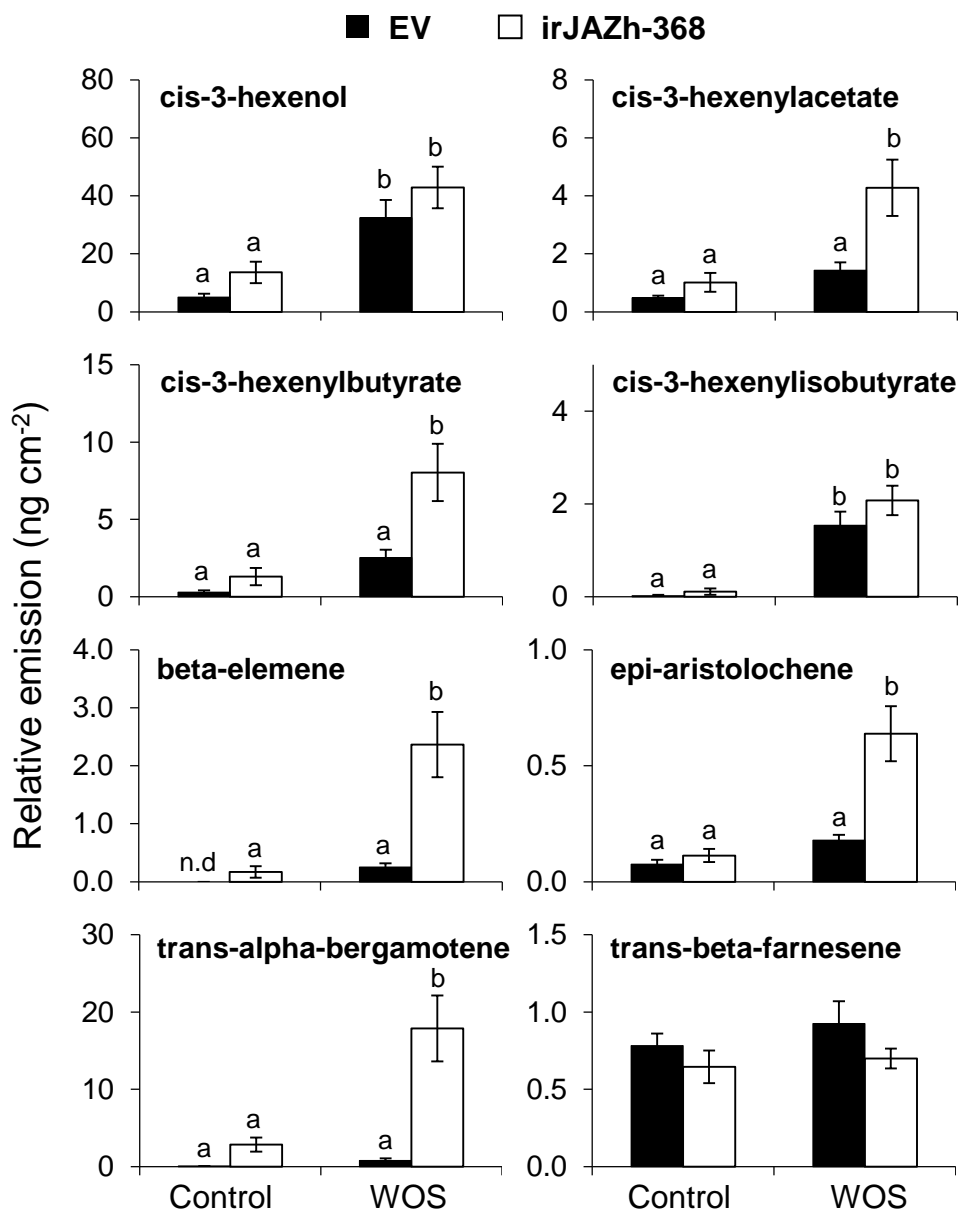
## 3. Single-malonylated DTGs



## 4. Di-malonylated DTGs



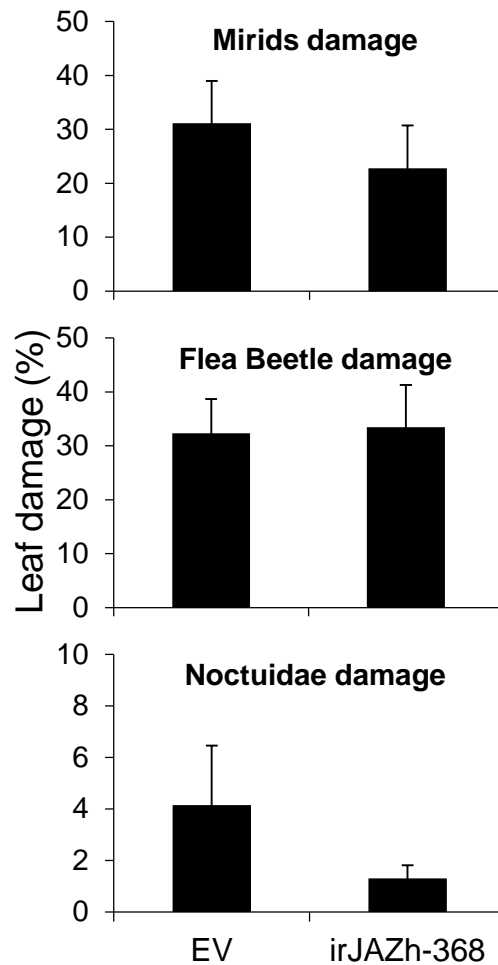
**Supplemental Figure S11.** Individual DTGs determined in EV and NaJAZh-silenced plants grown in the native habitat in Great Basin Desert, Santa Clara, Utah, USA. Mean  $\pm$  SE relative levels of individual DTGs ( $n=5$ ) measured in the leaves in native environment were consistently higher in W+OS-elicited irJAZh plants compared to EV plants (measured by LC-ESI-MS/MS). Asterisks indicate significant differences between EV and irJAZh plants determined by Student's t-test at each individual time point of measurement (\* $P \leq 0.05$ , \*\* $P \leq 0.01$ , \*\*\* $P \leq 0.001$ ). FM, fresh mass.



**Supplemental Figure S12.** Volatile emission rates of EV and irJAZh plants grown in the native habitat in Great Basin Desert, Santa Clara, Utah, USA. irJAZh plants emitted larger amounts of volatile organic compounds (VOCs) and green leaf volatiles (GLVs) in native environment: VOCs and GLVs were determined by GC-MS after 24 h field trapping of volatiles from locally treated leaf (W+OS) using charcoal filters with an open-flow trapping system that pulled air from the headspace of the leaf through the trap with a vacuum pump connected to a car battery.

**Supplemental Figure S10.** (continued)

irJAZh plants emitted significantly larger amounts of the sesquiterpenes, beta-elemene, epi-aristolochene and trans-alpha-bergamotene, but similar amounts of trans-beta-farnesene as determined by GC-MS. Bars indicate the emission rates of volatiles  $\pm$  SE that were normalized to the internal standard, tetralin, added at the beginning of extraction process ( $n=9$ ). Asterisks indicate significant differences between EV and irJAZh plants determined by Student's t-test (\* $P \leq 0.05$ , \*\* $P \leq 0.01$ ).



**Supplemental Figure S13.** Herbivore damage inflicted by the native herbivore community to EV and NaJAZh-silenced plants grown in *N. attenuata*'s native habitat in Great Basin Desert, Santa Clara, Utah, USA. EV and irJAZh-368 plants were planted in a size-matched paired- design in the field plot and natural herbivore damage was scored throughout the 2011 field season. Mirid damage was determined as the % of chlorotic damaged area of the total plant canopy caused by cell-damaging feeding of *Tupiocoris notatus* mirid bugs; flea beetle damage as the % of leaf canopy damaged by the small feeding holes that characterize flea beetle feeding; and Noctuidae damage as the % of leaf canopy lost due to leaf consumption by these Lepidopteran larvae.



**Supplemental Figure S14.** Diaminobenzidine (DAB) staining in the leaves from field-grown EV and irJAZh plants. NaJAZh-silencing induced higher accumulations of hydrogen peroxide in the leaves of field grown plants. Leaves were subjected to a standardized mechanical wound by puncturing leaves with a cork-borer immediately prior to placing detached leaves in the DAB solution. irJAZh plants showed darker brown circles around punctured areas; however the EV leaf staining was relatively stronger compared to a similar experiments conducted in the glasshouse (compare with Figure 10 in Text). Despite high levels of staining, neither EV nor irJAZh plants developed necrotic symptoms in the field (see Supplemental Figure S13 online).



**EV plant**



**irJAZh plant**



**Supplemental Figure S15.** Leaves of irJAZh and EV plants grown in native habitat of Great Basin Desert, Utah (USA). Despite high levels of DAB staining, neither EV nor irJAZh plants developed necrotic phenotype in the field. We planted 15 and 18 size-matched pairs of irJAZh and EV plants in the field in 2010 and 2011, respectively. Most of the plants were maintained in the field until the early flowering stage or later developmental stage (with periodically removed flowers); however, none of the leaves at any developmental stage of field-grown irJAZh plants showed necrosis.